Journal of Alloys and Compounds 509 (2011) 6152–6157

Contents lists available at ScienceDirect

Journal of Alloys and Compounds

journal homepage: www.elsevier.com/locate/jallcom

Textured zinc oxide prepared by liquid phase deposition (LPD) method and its application in improvement of extraction efficiency for 650 nm resonant-cavity light-emitting diode (RCLED)

Po-Hsun Lei*, Ming-Jun Ding, Yuan-Chih Lee, Meng-Jung Chung

Institute of Electro-Optical and Material Science, National Formosa University, No. 64, Wunhua Rd., Huwei, Yunlin County 632, Taiwan, ROC

A R T I C L E I N F O

Article history:
Received 6 December 2010
Received in revised form 25 February 2011
Accepted 6 March 2011
Available online 16 March 2011

Keywords:
Zinc oxide (ZnO)
Liquid-phase deposition (LPD)
Resonant-cavity light-emitting diodes (RCLEDs)

A B S T R A C T

In this article, we report on the textured zinc oxide (ZnO) prepared by liquid-phase deposition (LPD) method and apply it as a window layer of 650 nm resonant-cavity light-emitting diode to enhance the extraction efficiency. The treatment solution for LPD ZnO (LPD-ZnO) growth consists of ZnO powder saturated with hydrochloric acid (HCl) and hydrogen peroxide (H_2O_2). Temperature-controlled water bath system was used to maintain a constant temperature of 40 °C in LPD system. The experimental results indicate that the deposition rate was determined by the concentration of H_2O_2 and growth temperature, and the average roughness of LPD-ZnO is dominated by the concentrations of HCl. In order to perform the practicability of LPD-ZnO, the textured LPD-ZnO is used as a window layer of 650 nm AlGaInP/GaInP resonant-cavity light-emitting diode (RCLED) to enhance the light output power. In addition, the calculated results indicate that the optimum roughness for enhancing the light output power of RCLED is in the range of 80–100 nm, which are close to the experimental results. As compared to the conventional RCLED, the RCLED with textured LPD-ZnO, which has the optimum average roughness of 82 nm, performs a high light output power, a high external quantum efficiency, a narrow linewidth of electroluminescence spectrum and the same far-field angle.

1. Introduction

In the past decade, zinc oxide (ZnO) semiconductor materials with the high direct band-gap (~3.37 eV) and high exciton binding energy (~60 meV) have been attracted much attention in the applications for the functional window materials in laser diodes (LDs), light-emitting diodes (LEDs) and solar cell [1–3]. Several techniques such as chemical vapor deposition (CVD) [4,5], pulsed-laser deposition (PLD) [6], molecular-beam epitaxy (MBE) [7], sputtering [8], and hydrothermal method [9] were used for growth of ZnO film. Among them, CVD, especially metal-organic chemical vapor deposition (MOCVD), are the most popular technique to grow ZnO film due to that it directly creates a textured surface with strongly light scattering capacity. However, the substrate temperature should be heated above 200 °C to obtain a high-quality ZnO film by CVD techniques. Recently, liquid-phase deposition (LPD) method was reported to grow SiO_2 on Si substrate under a low growth temperature [10]. LPD technology takes advantages such as low growth temperature, low cost, large area growth, good step coverage, and simple deposition instrument.

In this article, we have grown ZnO textured film on GaAs substrate under the temperature about 40 °C by LPD method. The experimental results represents that the average roughness of LPD-ZnO films can be modulated by the concentration of hydrochloric acid (HCl) and the deposition rate of LPD-ZnO films can be controlled by the concentration of hydrogen peroxide (H_2O_2).

Recently, light sources in the telecommunication systems, such as fiber-to the home (FTTH) and low-cost parallel interconnects, are required of low cost, high-temperature sensitivity, high reliable and eye safe components. For these demands, high external efficiency, low temperature sensitivity, and low cost light emitting diodes (LEDs) are needed [11]. In 1946, Purcell [12] suggested that the spontaneous emission of a radiating system can be replaced by a so-called microcavity which has the dimension on the order of the emitted light wavelength. The microcavity can provide a redistribution of emitting light through the enhancement or inhibition of spontaneous emission, depending on the position of the emission dipole with respect to the cavity-standing wave pattern. LEDs with the microcavity can be named microcavity light-emitting diodes (MCLEDs) or resonant-cavity light-emitting diodes (RCLEDs). They consisted of three parts, including a multiple-quantum-well active region, a microcavity, and two parallel mirrors surrounding the cavity. Due to the coupling of the quantum wells with Fabry–Perot cavity mode, the emitting wavelength of RCLEDs can be selected.

* Corresponding author. Tel.: +886 5 6315668; fax: +886 5 6329257.
E-mail address: pohsunlei@gmail.com (P.-H. Lei).

0925-8388/$ – see front matter © 2011 Elsevier B.V. All rights reserved.
doi:10.1016/j.jallcom.2011.03.039

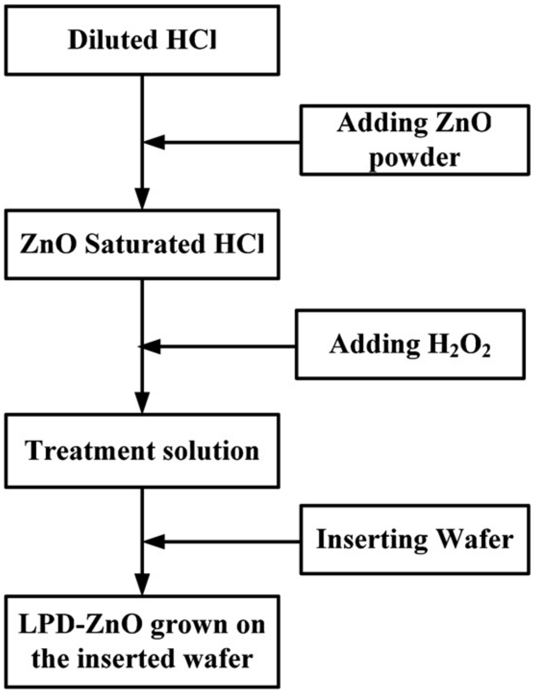

Fig. 1. Schematic flow chart for LPD-ZnO.

Recently, the 650 nm RCLEDs with a high output power and a narrow line width, which have low attenuations of 0.13–0.18 dB/m [13,14] in red-wavelength region, can be applied to optical communication system, such as FireWire or i. Link (IEEE 1394b) in polymethyl-methacrylate (PMMA) plastic optical fiber (POF). Royo et al. [15] presented the analytical and numerical calculation of the extraction efficiency for RCLEDs by the first derivative of the distributed Bragg reflectors (DBRs) phase with respective to the angle and energy at the Bragg condition, and by approximations of the amplitude and phase of the complex reflection coefficients through a constant and first-order Taylor development. Due to a redirection of the Airy mode inside the escape window, the RCLEDs have higher extraction efficiency than the conventional LEDs. Streubel et al. [16] indicated that RCLEDs have an extraction efficiency of one order in magnitude stronger than the conventional planar LEDs, and this result has been proven in many literatures [17–19]. In order to perform the practicability of LPD-ZnO, the textured LPD-ZnO film was applied to AlGaInP/GaInP resonant cavity light emitting diodes (RCLEDs) to meliorate the extraction efficiency. The random texturing improves light extraction via efficient surface randomization where photons emitted out of an escape cone have increased [20]. According to the calculated results, the optimum average roughness of textured LPD-ZnO for enhancing light output power of 650 nm RCLED is around 82 nm. As compared to that of RCLED without LPD-ZnO textured window layer, RCLED with LPD-ZnO textured window layer showed an improvement of 26% and a decrease of 13.5% in light output power and FWHM of emission spectra, respectively.

2. Experimental details

The schematic flow chart of ZnO film prepared by LPD method is shown in Fig. 1. The treatment solution to grow textured LPD-ZnO film was prepared by the following steps. First, 50 ml HCl (12 M, Taimax) was diluted with deionized (DI) water to 1.72 M, 2.01 M, 2.412 M, and 3.015 M, respectively. Second, the diluted HCl solution was stirred with the ZnO powder (J. T. Baker) for 1 h at 25 °C to ensure that HCl is saturated with ZnO powder. Third, the undissolved ZnO powder was removed by the filtration. Finally, the 1 ml H_2O_2 (Taimax) solution with the different concentrations including 1.02 M, 1.13 M, 1.27 M, 1.7 M, 2.55 M, and 5 M, was added to the ZnO-saturated HCl solution to form the treatment solutions. The LPD-ZnO deposition system contains a Teflon vessel immersed in a temperature-controlled water bath system, which can offer a uniform temperature distribution by the cyclic water with the accuracy of 0.1 °C. In LPD-ZnO growth process, the Teflon vessel contained treatment solution should immerse in the temperature-controlled water bath system for 3–5 min at the setting growth temperature. This preheated step can guarantee the uniformity of the roughness of the ZnO film grown on the inserted substrate. Then, the (1 0 0)-oriented GaAs substrate with doping Si concentration of 1×10^{18} cm^{-3} was inserted in the treatment solution for LPD-ZnO growth.

The device structure of the 650 nm AlGaInP/GaInP RCLED consists of (i) a 0.5 μm n-GaAs buffer layer, (ii) 32-pair Si-doping AlGaAs/AlAs n-type DBR layers, (iii) a 32.8 nm n-type doping $(AlGa)_{0.7}In_{0.3}P$ waveguide layer, (iv) a 41.8 nm undoped $(AlGa)_{0.5}In_{0.5}P$ layer, (v) an active region composed of three 8 nm undoped GaInP wells separated by two 11 nm undoped $(AlGa)_{0.5}In_{0.5}P$ quantum barriers, (vi) a 41.8 nm undoped $(AlGa)_{0.5}In_{0.5}P$ layer, (vii) a 32.8 nm p-type doping $(AlGa)_{0.7}In_{0.3}P$ waveguide layer, (viii) 8-pair C-doping AlAs/AlGaAs p-type DBR layers, and (ix) a 0.01 μm p^+-GaAs ohmic layer. The uniformity of the epitaxial wafer is in term of photoluminescence (PL) intensity and FWHM, and the thickness is controlled within 5% across the 3-inch-in-diameter epitaxial wafer. The contact metal for device was composed of Ti/Pt/Au.

The thickness of LPD-ZnO film was measured by the field-emission scanning-electron microscope (FE-SEM) and the average roughness of LPD-ZnO film was analyzed by atomic force microscope (AFM) (D13100, Digital instruments Veeco Metrology Group). The typical light output power-current-voltage (*L–I–V*) measurements were performed by using a current measured unit and a calibrated power meter (Keithley 2520). The emission spectra were detected by Optical Spectrum Analyzer (ADCMT 8341). The far-field angle was found by profile meter (HIGHER WAY).

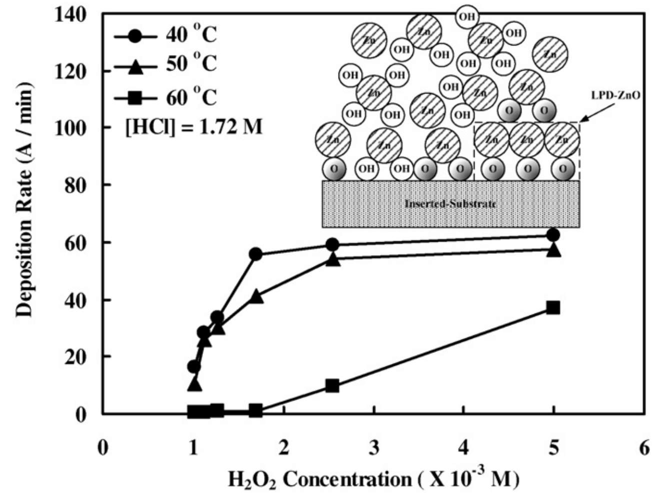

Fig. 2. The growth rate of LPD-ZnO as a function of H_2O_2 concentration at deposition temperature of 40, 50, and 60 °C. The inset represents the growth mechanism.

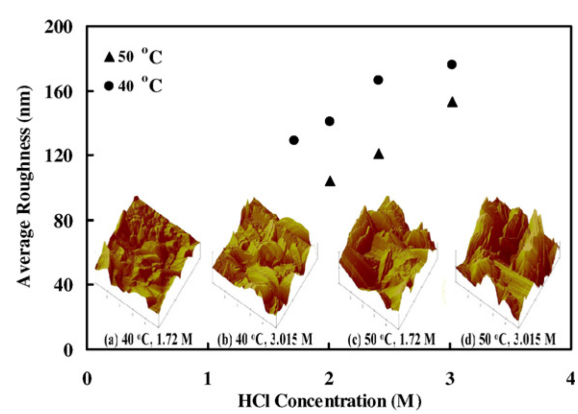

Fig. 3. The average roughness of LPD-ZnO as a function of HCl concentration at deposition temperature of 40 and 50 °C. The inset shows the AFM microscope.

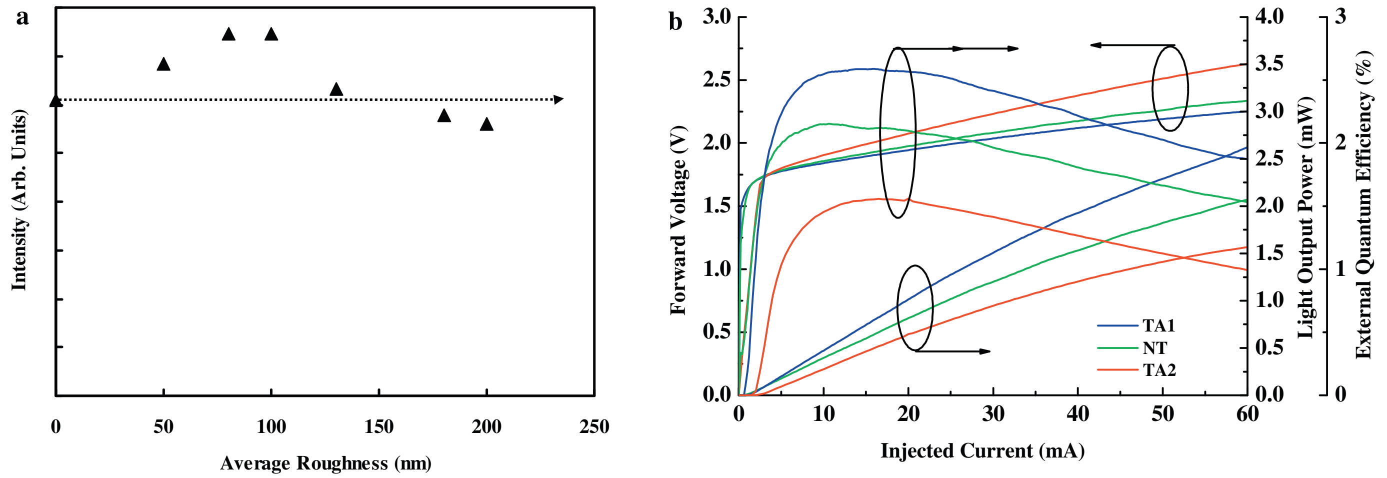

Fig. 4. (a) The calculated light output power (in arb. units) of 650 nm RCLED as a function of roughness of textured window layer and (b) the measured light output power, forward voltage, and external quantum efficiency as a function of injection current.

3. Results and discussion

3.1. Growth of LPD-ZnO

Fig. 2 shows the deposition rate of LPD-ZnO as a function of H_2O_2 concentration at different deposition temperatures. The concentration of HCl was 1.72 M and the concentrations of H_2O_2 were 5×10^{-3} M, 2.55×10^{-3} M, 1.7×10^{-3} M, 1.27×10^{-3} M, 1.13×10^{-3} M, and $1.0\ 2 \times 10^{-3}$ M, respectively. As can be seen in Fig. 2, the deposition rate rises dramatically in the concentration range of H_2O_2 between 1.02×10^{-3} and 1.7×10^{-3} M and represents a gradual change for the concentration over 1.7×10^{-3} M. The chemical reaction for ZnO-saturated HCl solution can be expressed as:

$$ZnO + 2HCl \Leftrightarrow Zn^{2+} + 2Cl^- + H^+ + OH^- \quad (1)$$

The high-concentration zinc species in ZnO-saturated HCl solution, including ZnOOH, $Zn(OH)_4{}^{2-}$, and $ZnO_2{}^{2-}$, lead the following reactions to the growth of ZnO [21].

$$Zn(OH)_4{}^{2-} \Leftrightarrow Zn(OH)_2 + OH^- \quad (2)$$

$$Zn(OH)_2 \Leftrightarrow 2H^+ + ZnO_2{}^{2-} \quad (3)$$

$$Zn^{2+} + 2ZnO_2{}^{2-} \Leftrightarrow ZnO \quad (4)$$

Eqs. (1)–(4) can be summarized by saying that during a ZnO growth experiment under liquid-phase condition one might have the following transport of Zn-containing species from the powder to thin film:

$$ZnO\ \ (\text{powder}) + HCl + H_2O_2 \rightarrow Zn(OH)_4{}^{2-} \rightarrow Zn(OH)_2 \rightarrow ZnO_2{}^{2-} \rightarrow ZnO \quad (5)$$

Eq. (5) indicates that ZnO deposition rate strongly depends on the concentration of $Zn(OH)_4{}^{2-}$, $Zn(OH)_2$, and $ZnO_2{}^{2-}$. In order to increase the deposition rate at a low deposition temperature, weak-acid H_2O_2 was used to reduce the concentration of OH^- ion in Eq. (2), hence a movement from left to right occurred, which caused an increasing concentration of $Zn(OH)_2$. The high-concentration $Zn(OH)_2$ led a movement from left to right in Eq. (3), and therefore the concentration of $ZnO_2{}^{2-}$ rised. The high-concentration $ZnO_2{}^{2-}$ can foster the growth of ZnO and thus the growth rate of LPD-ZnO increases with increasing the concentration of H_2O_2. The schematic growth mechanism is shown in the inset of Fig. 2. However, further increasing the concentration of H_2O_2 over 1.7 M, a gradual change in deposition rate was found. This phenomenon might be attributed to that the concentration of H^+ ions in the treatment solution increased with further increasing the concentration of H_2O_2, which caused a reduced concentration of $Zn(OH)_2$ as can be seen in Eq. (3). In addition, the deposition rate also decreases with increasing the deposition temperature. As the deposition temperature increases, the solubility of ZnO in HCl increases and therefore a ZnO-unsaturated HCl solution could cause a reduction of deposition rate.

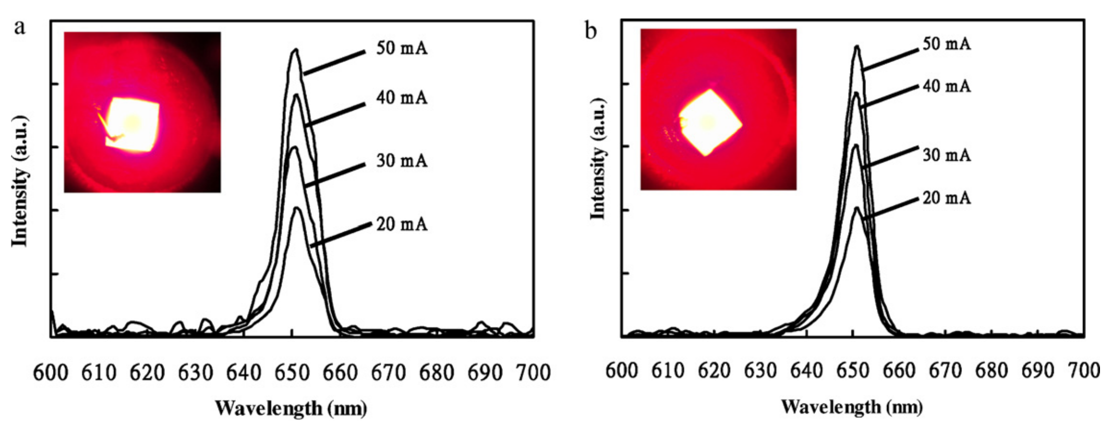

Fig. 5. The room-temperature electroluminescence (EL) spectra at forward currents of 10, 20, 30, 40 and 50 mA for RCLED (a) without textured LPD-ZnO and (b) with textured LPD-ZnO. The inset represents the light emission microscope.

Fig. 3 shows the measured average roughness as a function of HCl concentration at the deposition temperatures of 40 and 50 °C while the concentration of H_2O_2 maintained 1.13×10^{-3} M. The inset of Fig. 3 represents the AFM for the HCl concentration of 1.72 M and 3.015 M at deposition temperature of 40 and 50 °C, respectively. The average roughness for the deposition temperature of 40 °C is lower than that of 50 °C. This result can be explained as follow. LPD-ZnO grown at a low deposition temperature represents a poorly defined crystal orientation as well as amorphous morphology. The high deposition rate at 40 °C (see Fig. 2) brings a planar surface morphology of LPD-ZnO. In addition, the average roughness of LPD-ZnO also increases with increasing the HCl concentration due to etching of as-deposited LPD-ZnO in high HCl concentrations. In summary, the average roughness of LPD-ZnO was affected by deposition temperature and HCl concentration and the varied average roughness can be obtained by adjusting the concentration of HCl with proper concentration of H_2O_2 and deposition temperature.

3.2. AlGaInP/GaInP RCLED with textured LPD-ZnO

Finally, the textured LPD-ZnO applied to the window layer of 650 nm AlGaInP/GaInP RCLED to serve following functions: (1) the refractive index of LPD-ZnO is about 1.8, which can be used as an intermediate layer to alleviate the high internal total reflection of the interface between semiconductor and air; (2) the photons emitted from active region can be efficiently extracted by the textured window layer; and (3) unlike conventional texture technologies, which might result in unwanted surface states during the etching process, LPD-ZnO is not an etching process and therefore the surface states caused by etching process can be reduced. In principle, objects scatter light efficiently when the ration of the wavelength to the object dimension is between 1/10 and 2 [22]. In order to efficiently extract photons from the semiconductor to air, an optimum size of the scattering objects is very important. However, the optimum dimension of scattering object related to the ration of the wavelength is too wide, which would bring the complicated experimental processes. It is clear that suitable computation software is needed to avoid the unnecessary experiments. For this purpose, OptiFDTD computation software based on the finite-difference time-domain was used to calculate the light output power. In order to simplify the simulation process, two assumptions were considered. First, the photon escaped from active region through p-DBRs to window layer for the cases of RCLED with/without a textured window layer is equal. Second, the emitted photons are considered as a point-like source set in active region and the intensities of these sources satisfied the Gauss distribution. Fig. 4(a) represents the calculated output power of RCLED as a function of roughness of a textured window layer. The dot line represents the output power of RCLED without a textured window layer. The calculated results indicate that the maximum light output power occurred at the roughness of 80–100 nm. Further increasing or decreasing the roughness away from this range, the light output power will reduce. These results also satisfy the optimum dimension of objects between 1/10 and 2 [22]. Fig. 4(b) shows the measured forward voltage, light output power, and external quantum efficiency as a function of injection current for the AlGaInP/GaInP RCLED with and without textured LPD-ZnO. The chip size and diameter of emission window for all of the devices, including conventional and textured RCLED, are $300 \times 300\,\mu m^2$ and 250 μm, respectively. The conventional RCLED and RCLED with the average roughness of 82 nm and 166 nm are named as NT, TA1, and TA2, respectively in Fig. 4(b). The forward voltage V_F of NT, TA1 and, and TA2 biased at 20 mA are 1.944, 1.975, and 2.04 V, respectively. The V_F of TA1 and TA2 are higher than that of NT, which might result from the deterioration in ohmic contacts due to ZnO film growth on the periphery of the contact. In addition, the V_F of TA2 is higher than that of TA1. This phenomenon might be attributed to the etched interface between ZnO and RCLED caused by high HCl concentration in the treatment solution. Under an injection current of 20 mA, TA1 shows the highest light output power and represents an improvement of light output power by 26% as compared to that of NT. These results satisfy with the calculations shown in Fig. 4(a). The improvement of light output power is attributed to the textured LPD-ZnO, which can result in an high extraction efficiency due to more opportunities for the generated photons to reach the LPD-ZnO-semiconductor and LPD-ZnO-air interface within the angle of the escape cone. In addition, light output power of TA2 is lower than those of NT and TA1 because the light output power of RCLED depends on the roughness of the textured window layer as shown in Fig. 4(a). The external quantum efficiency is defined as [23]

$$\eta_{ext} = \frac{dP}{dI} \cdot \frac{\lambda e}{hc} = \eta_{int} \cdot \eta_{extraction} \quad (6)$$

where η_{ext}, η_{int}, and $\eta_{extraction}$ are the external quantum efficiency, internal quantum efficiency, and extraction efficiency, respectively, P is the photon power emitted to free space, I is the injection current, and λ is the wavelength of emitted photon. Due to the high extraction efficiency caused by the textured LPD-ZnO, TA1 represents the highest external quantum efficiency as compared to those of NT and TA2. Table 1 summarizes the measured forward voltage and light output power under an injection current of 20 mA for different chips adopted from TA1 sample. Due to the uniform average roughness of the textured LPD-ZnO, the forward voltage and light output power for each chip are almost equal (the variation of 3.5% for forward voltage and 0.6% for light output power).

Table 1
Summarize the forward voltage and light output power at an injection current of 20 mA for different chips adopted from TA1 sample.

Chip no.	Forward voltage @ 20 mA	Light output power @ 20 mA
1	1.962	1.849
2	1.978	1.852
3	1.886	1.857
4	1.961	1.851
5	1.94	1.845
6	1.869	1.866
7	1.868	1.859
8	1.919	1.854
9	1.868	1.857
10	1.86	1.861

Fig. 5(a) and (b) shows the room-temperature electroluminescence (EL) spectra at forward currents of 10, 20, 30, 40 and 50 mA for NT and TA1 and the inset of Fig. 5(a) and (b) represent the light emission microscope of NT and TA1 at an injection current 20 mA, respectively. The peak emission wavelength for NT and TA1 are found at 651 nm and is fairly constant with increasing current. This phenomenon indicates that the emission wavelength cannot be influenced by introducing the textured LPD-ZnO as a window layer. The FWHM for NT and TA1 in the preferential direction of emission spectrum are found as around 7.4 and 6.4 nm over the 10–50 mA current range. The FWHM for TA1 is smaller than that of NT, which might be attributed to that the textured-LPD-ZnO effectively diffracted the light in the preferential direction, resulting in the effective suppression of wavelength away from 650 nm [24].

Fig. 6(a) displays the far-field patterns of NT, TA1, and TA2, respectively. The lambertian emission pattern is given by [23]

$$I_{air} = \frac{P_{source}}{4\pi r^2} \frac{n_{air}^2}{n_m^2} \cos\theta \quad (7)$$

where P_{source} is the total output power from a point-like source, n_{air} and n_m are the refractive indices of air and window layer, respectively, and θ is the angle of incidence of the ray from the window

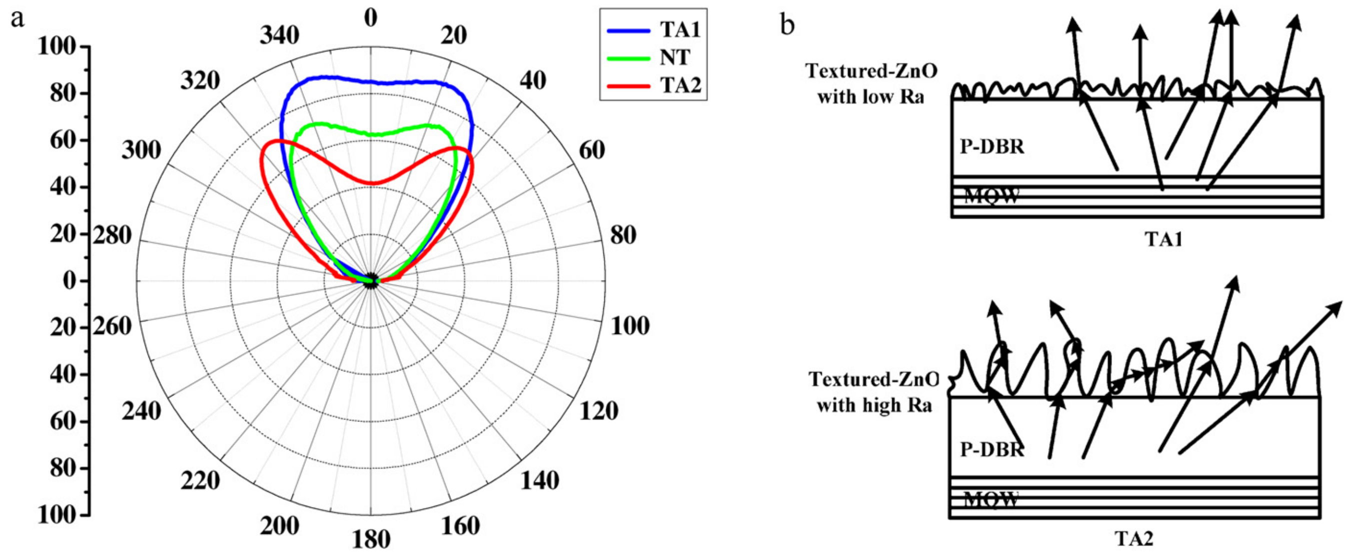

Fig. 6. (a) Radiation pattern of NT, TA1, and TA2, and (b) the schematic explanations of far-field angle for TA1 and TA2.

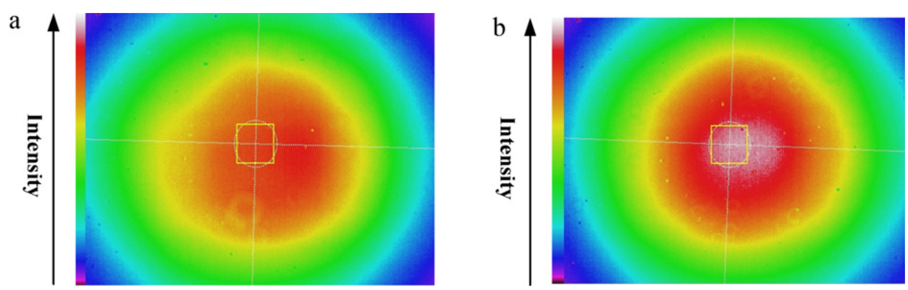

Fig. 7. Optical field pattern of RCLED (a) without textured LPD-ZnO and (b) with textured LPD-ZnO.

layer to air. It is clear that the lambertian emission pattern follows a cosine dependence and a high intensity can be obtained at the low angle of θ. TA1 represents a better directionality and a stronger luminous intensity at any emission angles than those of NT and TA2 due to the low angle of θ, which resulted from the optimum average roughness of textured LPD-ZnO. In addition, the high refractive index of LPD-ZnO (about 1.8) can be used as an intermediate layer between semiconductor and air to enlarge the critical angle of total internal reflection. Moreover, TA2 shows a wider far-field angle than those of TA1 and NT, which might be attributed to the larger angle of θ caused by the higher average roughness of LPD-ZnO. The schematic explanation for the photons emitted from high/low average roughness of textured LPD-ZnO is shown in Fig. 6(b).

Fig. 7(a) and (b) shows the 2-D optical field patterns for NT and TA1 at the driving current of 50 mA. As seen in Figs. 7(a) and (b), the white color region is found in the center of Fig. 7(b) while it is not found in Fig. 7(a). Moreover, the outline of Fig. 7(a) is more circular than that of Fig. 7(b). These results mean that TA1 with a high extraction efficiency and preferential diffracted direction represents a high intensity and a directional distribution optical field.

4. Conclusion

We have successfully prepared the textured ZnO by LPD method and applied it as a window layer of 650 nm RCLED to improve the extraction efficiency. The treatment solution for LPD-ZnO growth consisted of ZnO saturated with the hydrochloric acid (HCl) and hydrogen peroxide (H_2O_2). The deposition rate of LPD-ZnO is determined by the concentration of H_2O_2 and growth temperature and the average roughness of LPD-ZnO depends on the concentration of HCl. By using the textured LPD-ZnO as the window layer of 650 nm AlGaInP/GaInP RCLED, the extraction efficiency can be enhanced. The calculated and experimental results indicate that the optimum roughness for enhancing the light output power of RCLED is about 82 nm. As compared to the conventional RCLED, RCLED with textured LPD-ZnO represents a high light output power, a high external quantum efficiency, and a narrow electroluminescence spectrum while the far-field angle maintained a constant radiation pattern.

Acknowledgement

Financial support from the National Science Council (NSC 98-2622-E-150-004) is deeply appreciated.

References

[1] M.H. Huang, S. Mao, H. Feick, H. Yan, Y. Wu, H. Kind, E. Weber, R. Russo, P. Yang, Science 292 (2001) 1897.
[2] X.Y. Kong, Z.L. Wang, Nano Lett. 3 (2003) 1625.
[3] W.J. Jeong, S.K. Kim, G.C. Park, Thin Solid Films 506–507 (2006) 180.
[4] J. Hu, R.G. Gordon, J. Appl. Phys. 72 (1992) 5381.
[5] H. Asahara, D. Takamizu, A. Inokuchi, M. Hirayama, A. Teramoto, S. Saito, M. Takahashi, T. Ohmi, Thin Solid Films 518 (2010) 2953.
[6] A.V. Singh, R.M. Mehra, N. Buthrath, A. Wakahara, A. Yoshida, J. Appl. Phys. 90 (2001) 5661.
[7] T. Ohgaki, N. Ohashi, H. Kakemoto, S. Wada, Y. Adachi, H. Haneda, T. Tsurumi, J. Appl. Phys. 93 (2003) 1961.
[8] J.O. Barnes, D.J. Leary, A.G. Gardon, J. Electrochem. Soc. 127 (1980) 1636.
[9] J.H. Yang, J.H. Zheng, H.J. Zhai, X.M. Yang, L.L. Yang, Y. Liu, J.H. Lang, M. Gao, J. Alloys Compd. 489 (2010) 51.

[10] H Nagayama, H. Honda, H. Kawahara, J. Electrochem. Soc. 135 (1988) 2013.
[11] R. Bockstaele, C. Sys, J. Blondelle, B. Dhoedt, I. Moerman, P.V. Daele, P. Demeester, R. Baets, IEEE Photon. Technol. Lett. 11 (1999) 158.
[12] E.M. Purcell, H.C. Torrey, R.V. Pound, Phys. Rev. 69 (1946) 37.
[13] M. Saarinen, V. Vilokkinen, M. Dumitrescu, M. Pessa, IEEE Photon. Technol. Lett. 13 (2001) 10.
[14] S.J. Chang, C.S. Chang, IEEE Photon. Technol. Lett. 10 (1998) 772–774.
[15] P. Royo, R.P. Stanley, M. Ilegems, IEEE J. Selected Topics Quantum Electron. 8 (2002) 207.
[16] E.F. Schubert, Y.H. Wang, A.Y. Cho, L.W. Tu, G.J. Zydzik, Appl. Phys. Lett. 60 (1992) 921.
[17] G. Bjork, S. Machida, Y. Yamamoto, K. Igata, Phys. Rev. A 44 (1991) 669.
[18] H. De Neve, J. Blondelle, R. Baets, P. Demeester, P. Van Daele, G. Borghs, IEEE Photon. Technol. Lett. 7 (1995) 287.
[19] J.J. Wierer, D.A. Kellogg, N. Holonyak, Appl. Phys. Lett. 74 (1999) 926.
[20] W.C. Peng, Y.C.S. Wu, Appl. Phys. Lett. 89 (2006) 04116–4121.
[21] T. Yao, S.K. Hong, Advance in Material Research 12 Oxide and Nitride Semiconductors Processing, Properties and Applications, Springer, 2009.
[22] I. Schnitzer, E. Yablonovitch, C. Caneau, T.J. Gmitter, A. Scherer, Appl. Phys. Lett. 63 (1993) 2174.
[23] E. Fred Schubert, Light-emitting Diodes, 2nd ed., Cambridge University Press, 2006.
[24] Y.J. Lee, H.C. Kuo, S.C. Wang, T.C. Hsu, M.H. Hsieh, M.J. Jou, B.J. Lee, IEEE Photon. Technol. Lett. 17 (2005) 2289.